UNITED NATIONS EDUCATIONAL, SCIENTIFIC AND CULTURAL ORGANIZATION
INTERNATIONAL ATOMIC ENERGY AGENCY
INTERNATIONAL CENTRE FOR THEORETICAL PHYSICS
I.C.T.P., P.O. BOX 586, 34100 TRIESTE, ITALY, CABLE: CENTRATOM TRIESTE

H4.SMR/994-24

SPRING COLLEGES IN COMPUTATIONAL PHYSICS

19 May - 27 June 1997

ATOMIC CALCULATIONS AND PSEUDOPOTENTIALS

A. QTEISH
Center for Theoretical and Applied Physics
Yarmouk University
Irbid, JORDAN

lecture 1

Atomic Calculations and Pseudopotentials

Abdallah Qteish
Center for Theoretical and Applied Physics, Yarmouk University, Irbid-Jordan

Outline of the first lecture

- *Background.*
- *Pseudopotential theory.*
- *Justification of the pseudopotential theory.*
- *Norm-conserving pseudopotential generation (Kerker scheme).*
- *Atomic calculations*

Outline of the second lecture

- *Pseudopotential transferability*
- *The separable (Kleinman-Bylander) form.*
- *Pseudopotential optimization.*
- *Real space implementation of the non-local pseudopotentials.*
- *Non-linear exchange-correlation core corrections.*

Background

The electronic states can be separated into:

- Core: *highly localized; not affected by the chemical environment.*
- Valence: *extended; responsible for the chemical binding.*
- Semicore: *localized; slightly affected by the valence electrons; contribute to the chemical binding.*

Example: ZnS compound

Atomic energy levels (Ry)

state	Zn		S	
1s	-690.078	Core	-175.595	core
2s	-83.194		-15.414	
2p	-73.429		-11.517	
3s	-9.282		-1.269	valence
3p	-6.181		-0.529	
3d	-0.932	semicore		
4s$^{1.14}$	-0.532	valence		
4p$^{0.86}$	-0.158			

Solid Conf. TB cal.

Frozen core approximation: the core states are not allowed to relax - a common approximation in the pseudopotential and all-electrons approaches. ⇒ Very good approximation $\Delta E \sim 0.01$ eV.

The semicore electrons may be treated as valence states or as part of the frozen core: depending on the required accuracy and their degree of localization.

Nature of the valence wavefunctions (ψ_v): Show an oscillatory behavior inside the core region, due to their orthogonalization to the core states.

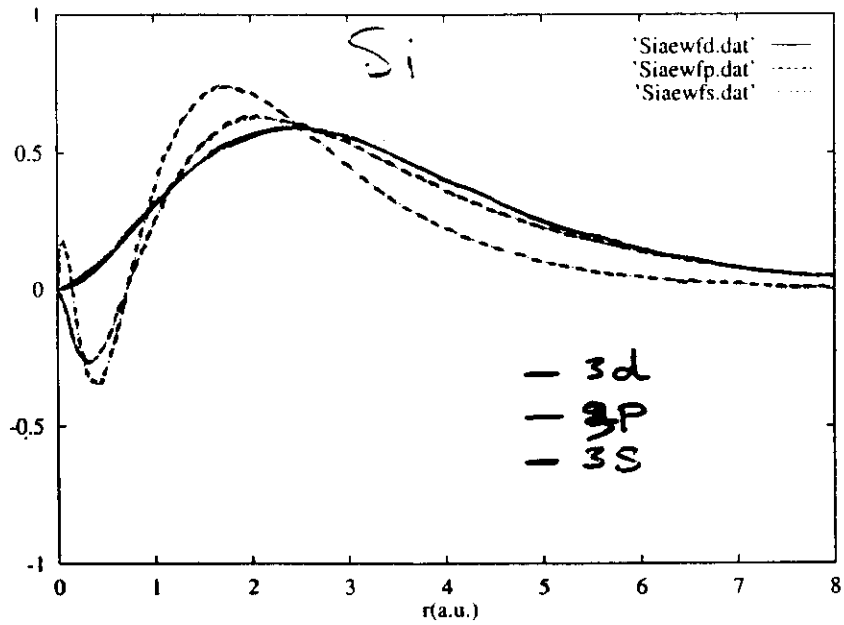

ψ_v is very difficult to expand in terms of plane-wave (PW) basis: huge numbers of PWs are required.

The actual shape of ψ_v inside the core region has negligible effects on the chemical binding between atoms, which is govern by the overlapping tails of ψ_v.

Pseudopotential Theory (Hellman, 1935).

Within the pseudopotential theory the core electrons are removed from the calculations and the orthogonalization of the of the valence states to the core ones is replaced by a "*repulsive potential*".

The pseudopotential (which is usually *l*-dependent) is the effective potential seen the valence electrons. In case of the atom, each of the *l*-component should give the valence *l*-state as its first eigenstate (*l*=0 to 2 or 3).

Example:

	core	valence
True Si atom	: $(1s^2\ 2s^2\ 2p^6)$	$(\ 3s^2\ 3p^2\ )$
		ε_{3s} ↕ ↕ ε_{3p}
Pseudo- Si atom :	.....	$1s^2\ 2p^2$

The Si *s*-pseudopotential must give the Si 3s eigenvalue as its lowest energy eigenvalue, and similarly for the other component.

Advantages of the pseudopotential approach:

- *It allows us to do accurate calculations for the valence electrons and the properties related to them, without the need to worry about the core electrons.*
- *The pseudo-wavefunction are smooth (nodeless), and so they can be expanded in terms a PW basis set.*

PW basis set

Advantages

- *The mathematical formulation is particularly simple.*
- *The basis sets are independent of the ionic positions.*
- *Allow the use of FFT.*
- *Convergence can be easily checked and improved.*

Shortcomings:

- *Very large numbers of PW are required in the solid state calculations in case of sharply peaked* ψ_v *(such as the d-and p-wavefunctions in transition metals and first raw elements, respectively)*

  This has been largely solved by:

  (1) Pseudopotential optimization..

  (2) Using very efficient total energy minimization methods, such as conjugate gradient method (Teter, Payne and Allan (89); Qteish (95)).
- *The PW basis sets are much less informative than the LCAO basis sets. However, a projection procedure has been recently introduced (Sanchez-Portal et al., J. Phys: Condens. Mat. (96)).*

8, 3859

Formal Justification (Phillips and Kleinman, 1959)

- Let ψ_v and ψ_c be the true valence and core wavefunctions of a certain Hamiltonian, H, or

  $$H\,|\Psi_i\rangle = \varepsilon_i\,|\Psi_i\rangle \text{ , with } i = v \text{ or } c.$$

- Let φ_v be smooth valence wavefunctions (not orthogonalized to the core states). Then,

  $$\Psi_v = \varphi_v - \sum_c \alpha_{cv}\Psi_c, \quad \text{where } \alpha_{cv} = \langle \Psi_c | \varphi_v \rangle.$$

- Now,

  $$H|\varphi_v\rangle = H\,|\Psi_v\rangle + H\sum_c \alpha_{cv}|\Psi_c\rangle$$

  or

  $$H|\varphi_v\rangle = \varepsilon_v\,(\,|\varphi_v\rangle - \sum_c \alpha_{cv}|\Psi_c\rangle\,) + \sum_c \alpha_{cv}\varepsilon_c|\Psi_c\rangle\,,$$

  So

  $$[\,H + \sum_c (\varepsilon_v - \varepsilon_c)|\Psi_c\rangle\langle\Psi_c|\,]\,|\varphi_v\rangle = \varepsilon_v\,|\varphi_v\rangle.$$

- Therefore, one can find an **exact** pseudo-Hamiltonian

  $$H^{PS} = H + \sum_c (\varepsilon_v - \varepsilon_c)|\Psi_c\rangle\langle\Psi_c|$$

  for which $|\varphi_v\rangle$ is an eigenstate with an eigenvalue ε_v.

Types of pseudopotentials

- Model or empirical pseudopotentials: *obtained through fitting of some calculated quantities to the corresponding experimental data.*
  - non-transferable.
  - Don't produce good electronic change density distributions.
- Ab-initio (parameter free) pseudopotentials: *constructed from first-principles atomic calculations -- highly accurate.*

Construction of ab-initio pseudopotentials

The LDA based ab-initio pseudopotentials are usually generated by imposing the following general conditions (Hamann, Schlüter and Chiang, 1979):

1. $\varphi(r)$ *is nodeless, and it is identical to the true wavefunction outside a suitably chosen core radius,* r_c.
2. $\varphi^{(n)}(r_c) = \Psi^{(n)}(r_c)$; *n=1 and 2.*

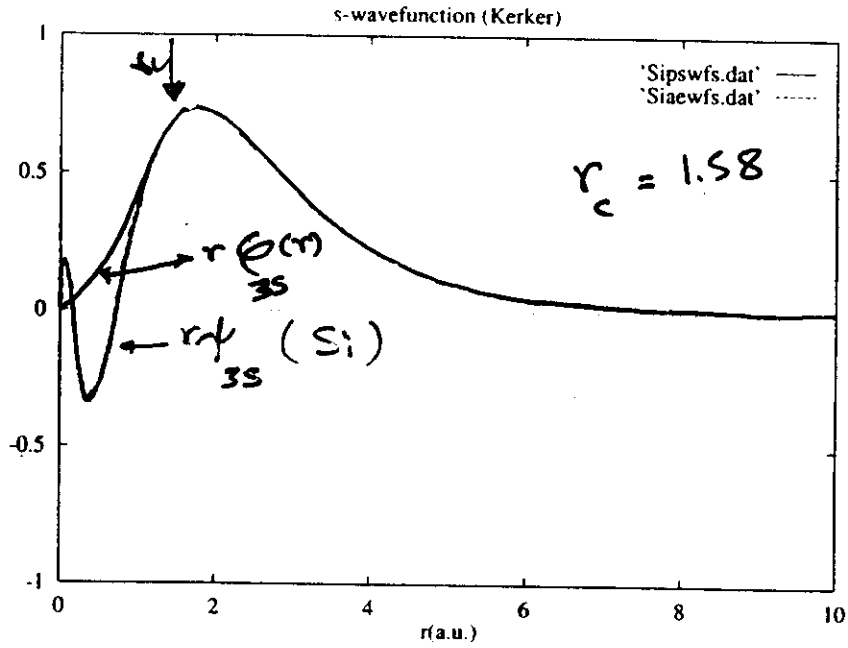

3. $\varepsilon_v^{PP} = \varepsilon_v^{AE}$.

4. $\int_0^{r_c} |r\varphi|^2 \, dr = \int_0^{r_c} |r\Psi|^2 \, dr$
   [norm-conserving condition].
5. *Other conditions to enhance the smoothness of the pseudpotentials.*

Several schemes have been proposed the generate ab-initio pseudopotentials which satisfy the above conditions. The most widely used are:

1- Hamann, Schlüter and Chiang (1979)
- *Bachelet, Hamann and Schlüter (1982).*
- *Vanderbilt (1985).*

2- Kerker (1980).

Kerker scheme

⇒The smooth pseudo-wavefunction inside the core region is given by

$$F(r) = r\varphi(r) = r^{l+1} e^{\alpha r^4 + \beta r^3 + \gamma r^2 + \delta}$$

⇒ α, β and γ can be determined analytically using conditions (1) to (3); whereas, δ is evaluated numerically from the norm-conserving condition. (For more details see Kerker's original paper).

⇒The screened pseudopotentials, $V_{PP}^{l,scr}$, are given by

$$V_{PP}^{l,scr}(r) = E + \lambda(2l + 2 + \lambda r^2) + 12\alpha r^2 + 6\beta r + 2\gamma \quad \text{, where}$$

$$\lambda = 4\alpha r^2 + 3\beta r + 2\gamma$$

Ionic pseudopotentials

- The *l*-components of the ionic pseudopotentials are then obtained by subtracting the screening potential due the valence electrons, or

$$V_l^{ion}(r) = V_{pp}^{l,scr} - V_H(n^v(r)) - V_{xc}(n^v(r))$$

- The ionic pseudopotential is usually given as

$$V^{ion}(r) = V_{loc}(r) + \sum_l V_l^{sl}(r) P_l ,$$

where

V_{loc} is a local potential, usually one of $V_l^{ion}(r)$.

$V_l^{ls} = V_l^{ion}(r) - V_{loc}(r)$ **{known as semi-local potentials}**

P_l is a projection operator.

This form takes care of the higher energy states than the ones considered.

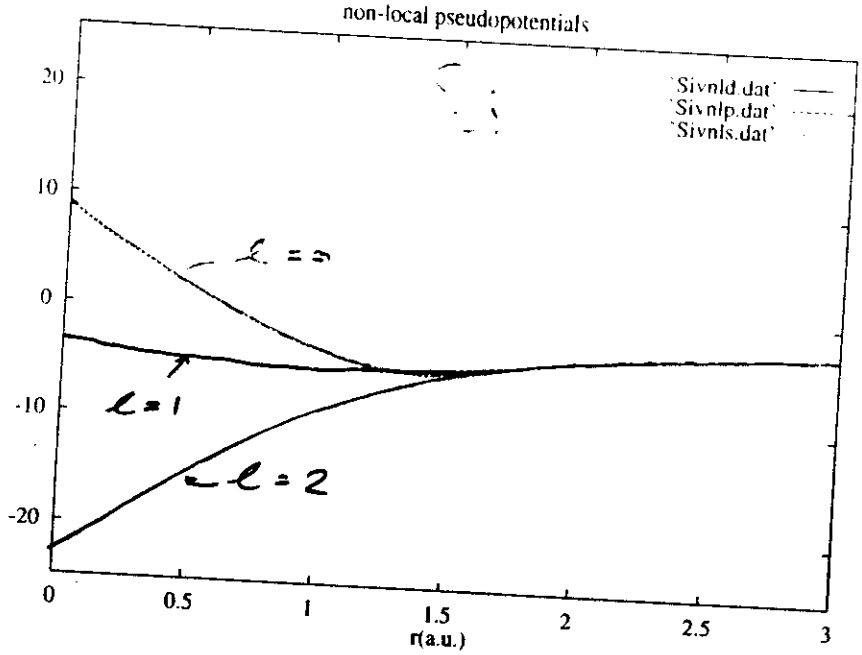

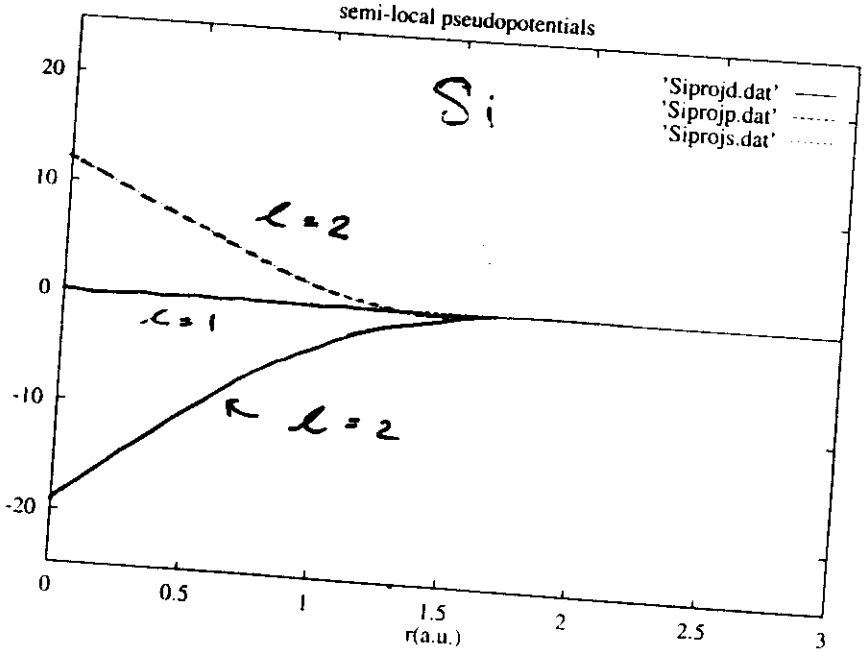

$$V_{loc}(r) = V^{ion}_{\ell=1}(r)$$

Self-consistent atomic calculations

- Using the LDA, the radial Sch. Eq. to solve is (a.u.)

$$[-\nabla^2 + V_{eff} + \frac{l(l+1)}{r^2}]P_{n,l} = \varepsilon_{n,l} P_{n,l} \ , \qquad (1)$$

where $V_{eff} = V_{nucl} + V_H + V_{xc}$,

in a logarithmic radial mesh.

- Self-consistent procedure:

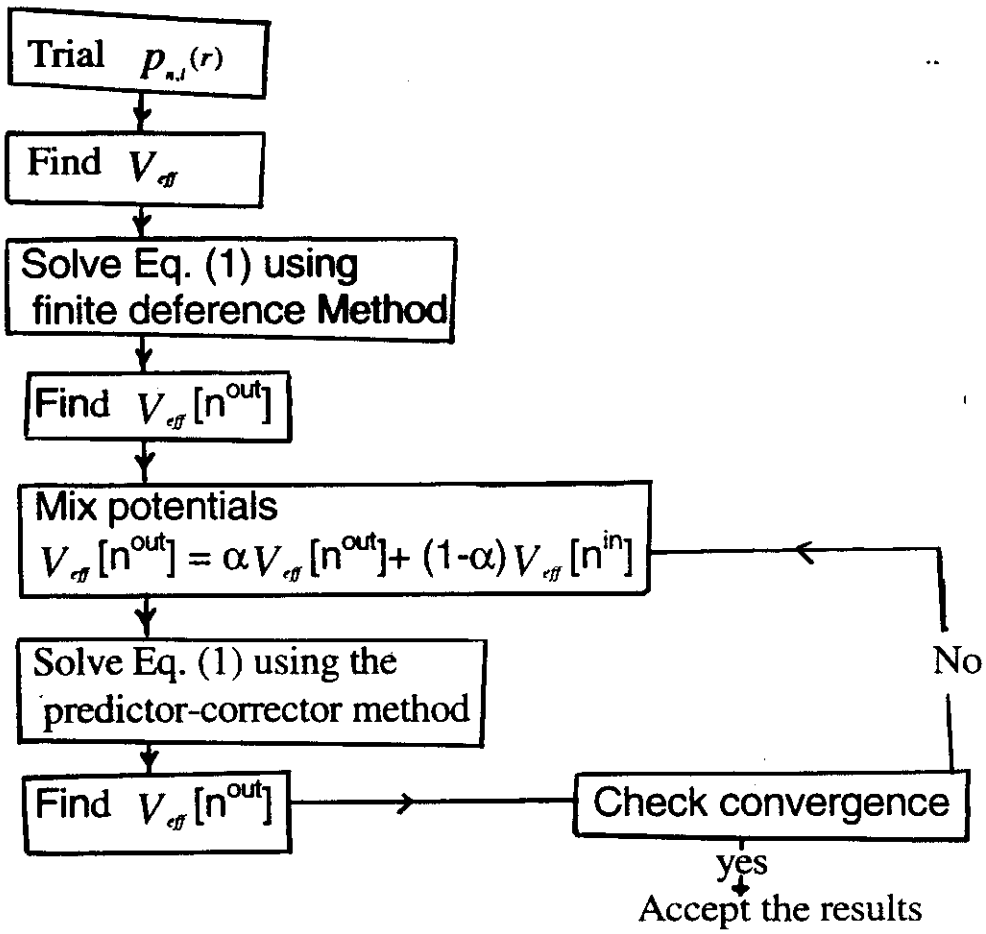

Transferability of the NC-PPs.

- The transferability of the generated PP can be checked by comparing its scattering properties with that of the true ionic potential.

- It is well known (see L. I. Schiff, Quantum mechanics, p 121) that the radial-logarithmic derivative of the l-partial wave at r_c is directly related to the scattering power of V_l.

- Now, it is worth showing that the NC condition ensures that the scattering properties of the corresponding PP is correct to first order in $(E - E_l)$, where E_l is the reference energy.
- To show this, let

$$x = P'/P \tag{1}$$

The Sch. Eq. can be rewritten in terms of x in the form

$$x'(r) + x(r)^2 = [V(r) + \frac{l(l+1)}{r^2} - E] \tag{2}$$

Differentiating Eq. (2) with respect to E, one gets

$$\frac{\partial x'(r)}{\partial E} + 2x(r)\frac{\partial x(r)}{\partial E} = -1. \tag{3}$$

Let $\frac{\partial x}{\partial E} = f$, then Eq. (3) becomes

$$\frac{\partial}{\partial r} f(r) + 2x(r)f(r) = -1. \tag{4}$$

Now, by making use of the relation

$$\frac{\partial}{\partial r} f(r) + 2x(r)f(r) = \frac{1}{p(r)^2}\frac{d}{dr}[p(r)^2 f(r)], \tag{5}$$

which valid for any function *f(r)*, multiplying by $p(r)^2$ and integrating between 0 and r_c, one arrives at

$$f(r_c) = \frac{\partial x(r_c)}{\partial E} = -\frac{1}{p(r_c)^2}\int_0^{r_c} p(r)^2 dr \,. \qquad (6)$$

- A good test for the transferability of the generated PP is to compare *x* for both the pseudo- and true wavefunctions over the energy range of interest.

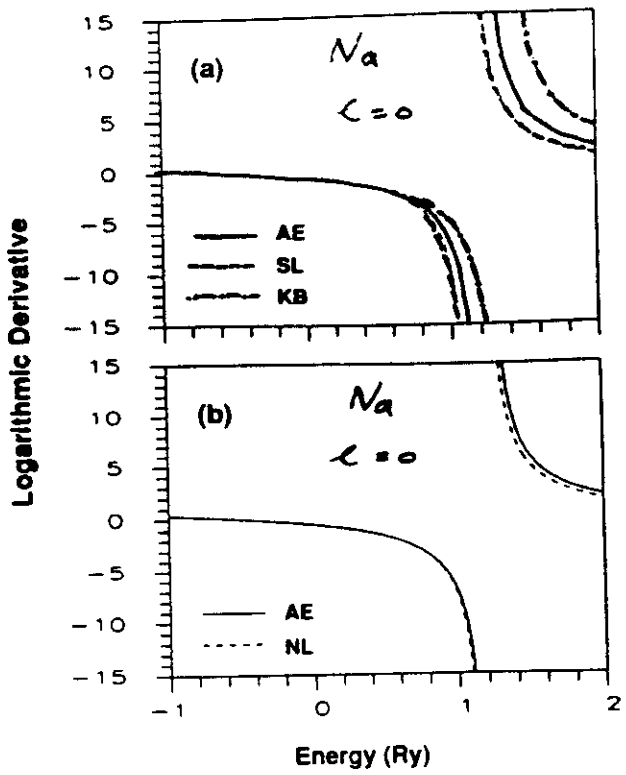

Chou
PRB 45, 11463 (92)

- As an alternative test, one can also compare the eigenvalues of several valence configurations (different from one from which the PP is generated) calculated using the generated PP with that obtained by solving the all-electrons Sch. Eq.

The Separable (Kleinman-Bylander) form

- Kleinman and Bylander [PRL **48**, 1425 (82)] have shown that the semi-local potential can be transformed to a truly non-local form. In this case, the ionic pseudopotential is given as

$$V^{nlm}(r,r') = V_{loc} + \sum_l E_l^{KB} Y_{lm}^*(\theta_{r'},\phi_{r'})\zeta_l(r)\zeta_l(r')Y_{lm}(\theta_r,\phi_r),$$

where, $E_l^{KB} = \dfrac{1}{\langle p_l V_l^{sl} | V_l^{sl} | V_l^{sl} p_l \rangle}$ and

$$\zeta_l(r) = V_l^{sl}(r)\, p_l(r). \qquad (8)$$

- To see the advantage of using the KB form, we note that

$$\langle e^{iq\cdot r} | Y_{lm} \rangle V_l^{sl} \langle Y_{lm} | e^{iq'\cdot r} \rangle \quad \alpha \quad \int j_l(qr) V_l^{sl} j_l(q'r) r^2 dr P_l(\theta_{qq'}).$$

(see Ihm, Zunger and Cohen, J. Phys. C 12, 4409 (79)), Whereas,

$$\langle e^{iq\cdot r} | \zeta_l \rangle \langle \zeta_l | e^{iq'\cdot r} \rangle \quad \alpha \quad \int j_l(qr)\zeta_l(r) r^2 dr \int j_l(q'r)\zeta_l(r) r^2 dr P_l(\theta_{qq'}),$$

which depends separately on q and q'.

- Thus, the KB form reduces the no. of integrals needed to be performed for each value of *l*, from N(N+1)/2 to just N. This particularly important in case of molecular dynamics simulations where the ionic configuration is frequently undated.
- The KB form also allows for the use of FFT, which leads also to a great reduction in the computational efforts needed in the electronic structure calculations of solids.

Ghost states

- When using the KB form one has to be very careful about his choice of V_{loc}, such that E_l^{KB} is never too large.
- If E_l^{KB} is too large, ghost (unphysical) states may develop below the true valence states, which ruins the solid state calculations.

Gonze et.al. PRB 41, 12264 (90)

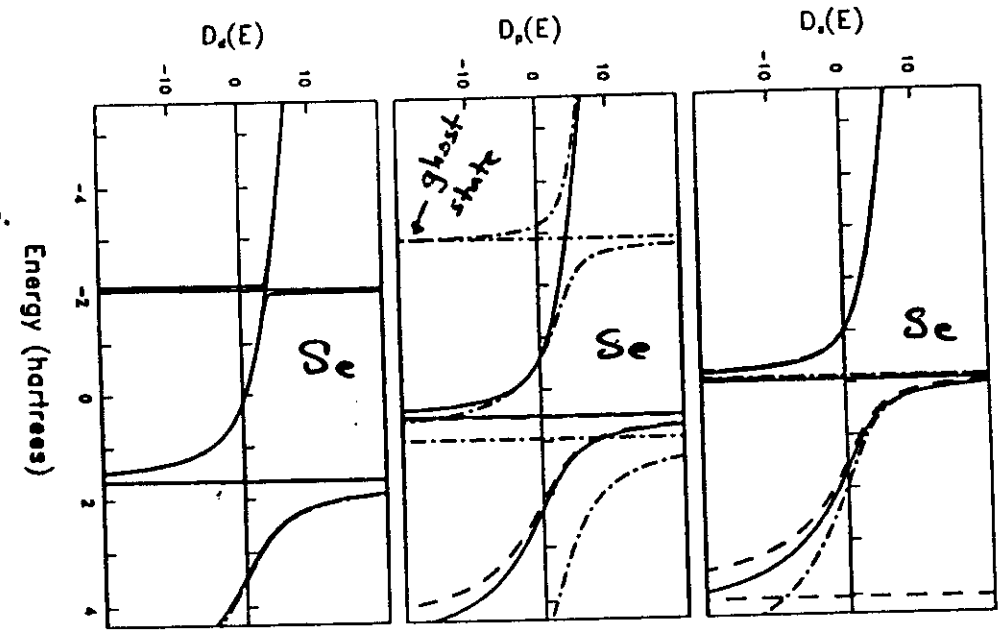

A ghost state test

Let E_l^{Loc0} and E_l^{Loc1} be the two lowest eigenvalues obtained from the self-consistent atomic potential without the non-local parts. Gonze, Stumpf and Scheffler [RB 44, 8503 (91)] have shown that

1. if $E_l<0$, a ghost state exists below E_l if and only if $E_l^{Loc0} < E_l$.
2. if $E_l>0$, a ghost state exists below E_l if and only if $E_l^{Loc1} < E_l$.

Generalized separable PP's.

Vanderbilt [PRB 41, 7892 (90)] and Blöchl [PRB 41, 5414 (90)] have shown that:

- The KB form of the PP can be directly obtained from the atomic calculations, without the help of V_l^{nl}, by noting that

$$|\zeta\rangle = (E_l - T - V_{loc})|p_l\rangle \qquad (9)$$

- The transferability of the separable PP can be highly improved by constructing $V_l(r,r')$ from two or more reference energies.

⇒Concentrating at one value of *l*, the pseudo-wavefunctions obtained at considered reference energies should satisfy the generalized NC condition $Q_{ij} = 0$, where

$$Q_{ij} = \int_0^{r_c} |r\ \psi_i|^2\, dr - \int_0^{r_c} |r\ \varphi_i|^2 dr \qquad (10)$$

⇒The generalized separable PP can be constructed as follows

1. Find the matrix $B_{ij} = \langle p_i|\zeta_j\rangle$, and invert it.
2. Define a new set of wavefunctions as $|\beta_i\rangle = \sum_j (B^{-1})_{ji}|\zeta_j\rangle$.
3. Then,

$$V^{nl}(r,r') = \sum_{i,j} B_{ij}|\beta_i\rangle\langle\beta_i|$$

⇒One can also easily show that

$(T + V_{loc} + V^{nl})|p_i\rangle = E_i|p_i\rangle$, for all values of E_i considered.

⇒ For further discussion about the generalized separable PP, see

1. Morrison, Bylander and Kleinman, PRB 47, 6728 (93).
2. Chou, PRB 45, 9837 (92).
3. Kresse and Hafner, J. Phys.: Condens. Matter 6, 8245 (94).

Pseudopotential Optimization

- The optimized pseudopotentials are the ones which lead to valence wavefunctions which converge rapidly in reciprocal space. This particularly important for transition metals and first row elements.
- Several schemes has been introduced to generate such optimized PP:
  1. The Rappe, Rabe, Kaxiras and Joannopoulos (RRKJ) approach [PRB 41, 1227 (90)].
  2. The Ultrasoft pseudopotentials of Vanderbilt [PRB 41, 7892 (90)]
  3. The Troullier and Martins approach [PRB 43, 1993 (91)].
- The first two approaches [which produce smoother PP's than the third one] will be discussed in some details below.

The RRKJ approach

- This approach is based on two observations:

  1. The convergence in momentum space of the atomic wavefunctions is transferable to that of the corresponding solids.

  2. For large energy cutoffs, the convergence of the total energy is similar to that of the kinetic energy contribution.

- Thus, by improving the convergence properties of the kinetic energy of the atomic wavefunctions an improved convergence of total energy of the solids can be achieved.

- The RRKJ scheme:

  1. Expand the already obtained pseudo-wavefunctions in the core region in terms of spherical Bessel functions

     $p_l(r) = \sum_{i=1}^{n} \alpha_i j_l(q_i r)$,

     where n is the no. of Bessel functions used.
  2. The values of q_i are obtained from $\frac{j_l(q_i r_c)}{j_l(q_i r_c)} = \frac{p_l'(r_c)}{p_l(r_c)}$.
  3. Choose a wavevector cutoff, q_c.
  4. Determine the values of α_i by minimizing

     $\Delta E_l(\alpha_1, \alpha_2, \ldots, q_c) = -\int_0^\infty d^3r\, p_l(r)\nabla^2 p_l(r) - \int_0^{q_c} d^3q q^2 |p_l(q)|^2$

- The Lin, Qteish, Payne and Heine [PRB 47, 4174 (93)] implementation of the RRKJ scheme:

  $n = 4$; $q_c = q_4$.

- Kresse and Hafner [J.Phys.:Condens. Matter 6, 8245 (95)] have argued that using only three Bessel functions leads even to smoother PP's than the ones generated using LQPH scheme. However, the transferability of these PP's is found to be rather bad, but it can be improved by using two reference energies.

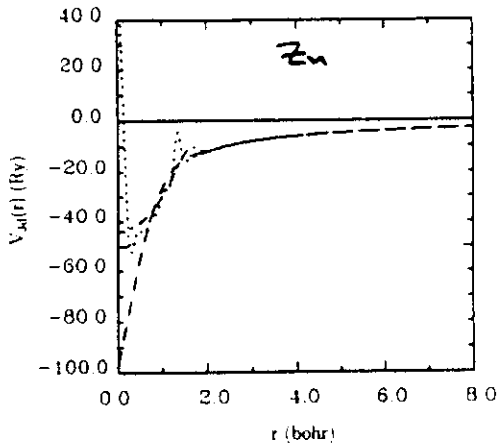

FIG. 2. Kerker pseudopotential (dashed line), optimized pseudopotential with $n=4$ and $q_c=q_4$ (dash-dotted line), and optimized pseudopotential with $n=10$ and $q_c=q_4$ (dotted line) generated for the Zn $3d$ eigenstate. The core radius is 2.00 bohr.

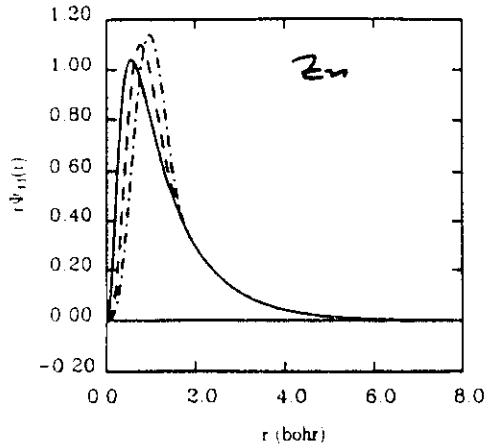

FIG. 3. All-electron wave function (solid line), Kerker pseudo-wave-function (dashed line), and optimized pseudo-wave-function (dash-dotted line) in real space for the Zn $3d$ eigenstate. The core radius is 2.00 bohr.

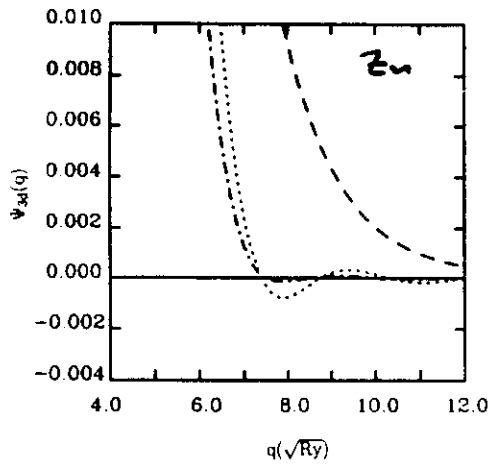

FIG. 1. Kerker pseudo-wave-function (dashed line), optimized pseudo-wave-function with $n=4$ and $q_c=q_4$ (dash-dotted line), and optimized pseudo-wave-function with $n=10$ and $q_c=q_4$ (dotted line) in Fourier space for the Zn $3d$ eigenstate with a core radius of 2.00 bohr.

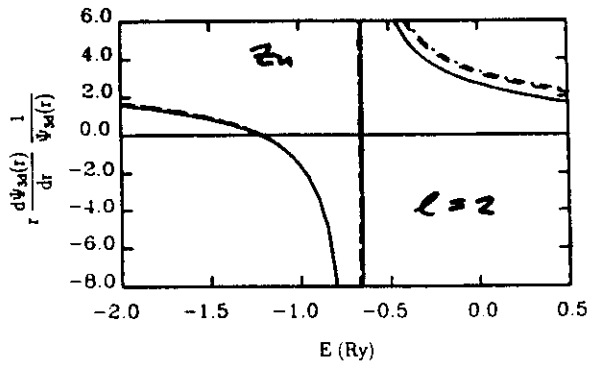

FIG. 4. The logarithmic derivatives of the all-electron radial wave function (solid line), Kerker (dashed line), and optimized (dash-dotted line) Kleinman-Bylander pseudo-wave-functions for $3d$ eigenstate of Zn with a core radius of 2.00 bohr. The atomic eigenvalue is $-0.912\,941$ Ry.

Lin et al. PRB 47, 4174 (1993)

Ultrasoft Vanderbilt Pseudopotentials

- Vanderbilt have shown that the generalized NC condition can be relaxed, which leads to ultrasoft (US)-PP's.

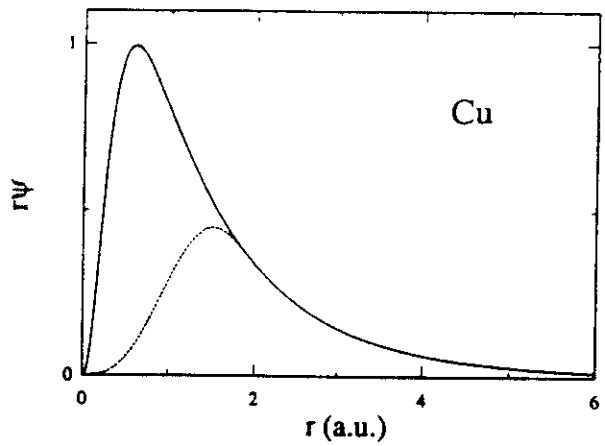

FIG. 1. All-electron (solid) and pseudo (dashed) radial wave functions of the 3*d* orbital of Cu. A cutoff radius of 2 a.u. has been used.

Laasonen et al.
PR B 47, 10142
(1993)

- In order to ensure the transferability of the US-PP's one has to adopt a generalized eigenvalue formalism

$$(T + V_{loc} + V_l^{US} - E\,S)\,|P_l\rangle = 0\,,$$

where, S is a Hermitian overlap matrix

$$S = 1 + \sum_{i,j} Q_{ij} |\beta_j\rangle\langle\beta_i|$$

- The US-PP's are, then, given as

$$V^{US} = \sum_{i,j} (B_{ij} + E_i Q_{ij}) |\beta_j\rangle\langle\beta_i|\,,$$

and the change density

$$n(r) = \sum_k f_k |p_k(r)|^2 + \sum_{k,i,j} f_k \langle p_k|\beta_j\rangle\langle\beta_i|p_k\rangle Q_{ij}\,.$$

Here, f_k is the occupation number of state *k*.

- The US-PP's require very small energy cutoffs (~ 20 Ry) even in the most difficult cases, such as Cu and C. However, the charge density augmentation process is quite involved and requires the use of two FFT grids one for the smooth part and one for the augmentation density. Thus, it is not a trivial matter to choose between the RRKJ and the US-PP approaches (which depends on several factors), but the US-PP approach is surely more efficient for systems with large unit cells. On the other hand, the RRKJ requires no changes in the existing codes.

Real-space implementation of the separable PP for first-principles electronic structure calculations.

- Can the non-local potential energy contribution, E^{nl}, be calculated also in real space?
- E^{nl} due to atom *i*, band *n* at a k-point in the first BZ, k, in real space is given by

$$E^{nl}_{i,n,k} = \sum_l \langle \Psi_{n,k} | V_l(r-\tau_i, r'-\tau_i) | \Psi_{n,k} \rangle$$

$$= \sum_l \sum_{m=-l}^{l} E_l^{KB} Z^*_{lm} Z_{lm}, \text{ where}$$

$$Z_{lm} = \int_{|r-\tau_i|<r_c} \zeta_l(r-\tau_i) Y_{lm}(\theta_{r-\tau_i}, \phi_{r-\tau_i}) \Psi_{k,n} d\,r \,. \qquad (10)$$

- Such process would require an O(mMP) operations, where m, M and P are no. of atoms per unit cell, no. of bands and no. of operations involved in calculating Z_{lm} (Eq. 10). This to be compared with O(mMN), where N, here, is the no.of PWs included.

- Calculating $E^{nl}_{i,n,k}$ using Eq. (10) is possible in principle, but it is not obvious in practice since $\Psi_{n,k}(r)$ are only known at the real-space FFT grid points.
- Now, Let

$$U_{lm} = \Omega_{mesh} \sum_{g} \zeta_l(g - \tau_i) Y_{lm}(\theta_{g-\tau_i}, \phi_{g-\tau_i}) \Psi_{k,n}(g) \,. \qquad (11)$$

be the value of Z_{lm}, but calculated only from the FFT grid points, g.

- Eq. (11) can transformed to

$$U_{lm} = \sum_{G} \sum_{\Gamma} \lambda_{lm}(\Gamma + G + k) \Psi_{n,k}(G) \,, \qquad (12)$$

where, Γ is the reciprocal lattice vectors of the g-grid points;

$$\lambda_{lm}(q) = \frac{4\pi i^l}{\sqrt{\Omega_{cell}}} \zeta_l(|q|) Y_{lm}(\theta_q, \phi_q) e^{iq.\tau_i} \,.$$

Here, $\zeta_l(q) = \int_0^{\infty} r^2 \zeta_l(r) j_l(qr) dr$.

- By comparing Eqs. 11 and 12 one can make the following two important observations.
  1. Errors are expected if the summation over Γ has to be performed [i.e., $\lambda_l(|q|)$ does not converge to zero for q of about $4G_{max}$, where G_{max} is the cutoff imposed on the PW expansion of the wavefunctions].
  2. U_{lm} does not depend on the value of $\lambda_l(|q|)$ for $G_{max} < q < \eta$, where η is about $3G_{max}$.
- King-Smith, Payne and Lin [PRB 44, 13063, (91)] have exploited these two points, and proposed the following scheme for calculating Z_{lm} using Eq. 11.

  1. Choose a suitable value for G_{max}.
  2. Introduce a new function $\chi_{l(|q|)}$ which is equal to $\zeta_l(|q|)$ for $0 < q < G_{max}$, and zero otherwise.

3. Select a cutoff radius in real-space, R_o, to be about 1.5 to $2r_c$.
4. Variationally find $\chi_{l(lq)}$ for $G_{max} < q < \eta$ by minimizing

$$I = \int_0^{R_o} |r\chi_l|^2 dr .$$

- Then $\chi_{l(r)}$ is used instead of $\zeta_{l(r)}$ is Eq. 11 to calculate Z_{lm}.

Si

$R_o = 1.8\ \text{Å}$

$r_c = 0.95\ \text{Å}$

$G_{max} = 7.24\ \text{Å}^{-1}$

$\eta = 17.85\ \text{Å}^{-1}$

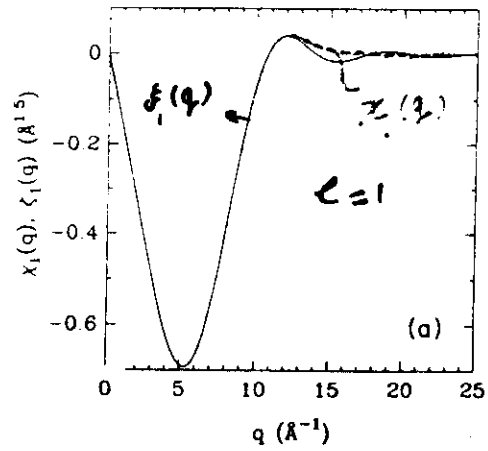

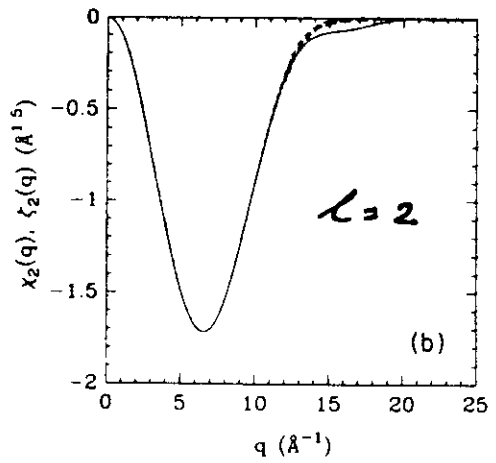

	Reciprocal space	Real space
Energy (eV)	−10.685 519 7	−10.685 513 9
Forces (eV/Å) atom no. 1		
x	1.290 944	1.290 895
y	1.290 942	1.290 892
z	1.290 944	1.290 894
Forces (eV/Å) atom no. 2		
x	−1.290 992	−1.291 024
y	−1.290 990	−1.291 022
z	−1.290 991	−1.291 024

King-Smith et al. PRB 44, 13063 (1991)

Non-linear exchange-correlation core corrections (NLCC)

- The unscreening process in the construction of the ionic PP's may involve some errors which reduces the transferability of these PP's. This is due to the fact that the exchange-correlation potential is not linear in terms of the charge density *n(r)*.

- If there is an overlap between $n^v(r)$ and $n^c(r)$, then
  $V_{xc}(n^v+n^c) \neq V_{xc}(n^v)+V_{xc}(n^c)$.
  This leads to a dependence of the ionic PP on $n^v(r)$.

- To overcome this difficulty, Louie, Froyen and Cohen [PRB 26, 1738 (82)] have suggested the following scheme

⇒ The following equation instead of the previously proposed one.

$$V_l^{ion}(r) = V_l^{scr}(r) - V_H - V_{xc}(n^v+n^c),$$

Moreover, $n^c(r)$ has to be added to $n^v(r)$ for the calculations of the XC energy or potential.

⇒ Since $n^c(r)$ does not converge rapidly in reciprocal space it can be replaced by

$$n^c_{partial} = \begin{cases} A\sin(Br)/r & \text{for } r < R_o \\ n^c(r) & \text{for } r > R_o \end{cases}$$

The parameters A and B are to be determined from the gradient of n^c at the cutoff radius R_o

⇒ The NLCC is found to give highly improved in many cases:
Example: the structural properties of ZnS.

on both sides of the equilibrium volume has been allowed. In Table I we show our calculated results for d, bulk modulus (B_0), and the pressure derivative of B_0 for both compounds, obtained by fitting the calculated total energies to Murnaghan's equation of state. The experimental data[33] and other similarly calculated values[34,35] (i.e., treating the semicore d electrons as valence states) are also shown. It is evident from Table I that the agreement between our results and the other theoretical ones is extremely good, and both are in excellent agreement with experiment. The calculated values of d and B_0 for the two compounds are within 1% and 10% of the corresponding experimental values, respectively. Such errors are of the same order as those in the corresponding LDA results, for III-V and group-IV materials.

Engel and Needs[36] have shown that the structural properties of ZnS can be significantly improved by including the nonlinear core corrections. The errors in their calculated d and B_0 were, respectively, about 4% and 37%, compared with 13% and 88% when the above corrections were not included. Our results shows that there is a clear further improvement over the results of Ref. 36, due to the relaxation of the semicore d electrons, which, in turn, indicates the important role of the latter on the calculated structural properties and bonding in II-VI compounds.

In Fig. 1, we show three-dimensional plots of the valence charge density, ρ, of ZnS in the plane of the bonds chain, and its decomposition into ρ_{sp} (calculated from the wave functions of the lowest and the three uppermost valence bands), and ρ_d (calculated from the wave functions of the occupied d bands) contributions. Both ρ_{sp} and ρ_d are properly symmetrized. The remarkable features to note are (i) the ρ_d is not spherically symmetric around the positions of the Zn ions, and that there is a

TABLE II. Energy levels (eV) at high-symmetry k points for ZnS, compared with the results of Martins, Troullier, and Wei (Ref. 34), calculated using a pseudopotential plane-wave (PP-PW) and linearized augmented plane-wave (LAPW) methods, and with the available experimental data.

Eigenvalues	Present work	Ref. 34 PP-PW	Ref. 34 LAPW	Experiment Ref. 33
Γ_{1v}	−13.21	−13.07	−13.11	−13.50
$\Gamma_{15v}(d)$	−6.65	−6.63	−6.55	~ −10.00
$\Gamma_{12v}(d)$	−6.17	−6.16	−6.09	~ −10.00
Γ_{15v}	0.00	0.00	0.00	0.00
Γ_{1c}	1.79	1.84	1.81	3.80
Γ_{15c}	6.21	6.15	6.19	8.35
X_1	−11.92	−11.77	−11.84	−12.00
X_{3v}	−4.77	−4.74	−4.70	−5.50
X_{5v}	−2.32	−2.29	−2.25	−2.50
X_{1c}	3.19	2.19	3.18	
X_{3c}	3.90	3.87	3.87	4.90
L_1	−12.24	−12.10	−12.16	−12.40
L_{1v}	−5.47	−5.43	−5.38	−5.50
L_{3v}	−0.92	−0.90	−0.88	−1.40
L_{1c}	3.30	3.05	3.05	
L_{3c}	6.78	6.75	6.76	

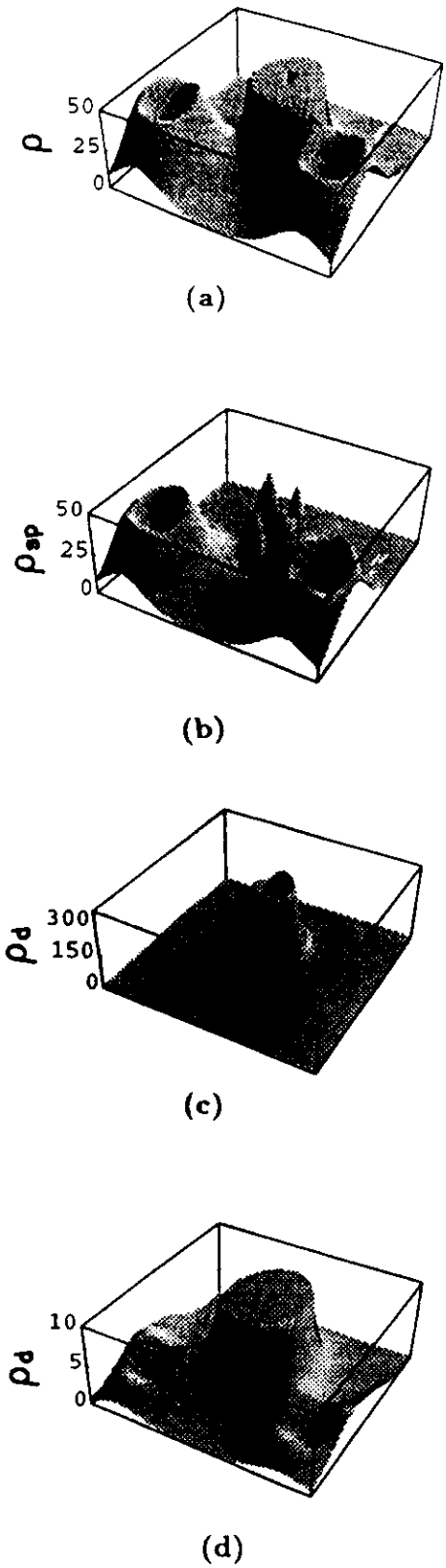

FIG. 1. Three-dimensional plots of the total charge density, ρ, of ZnS (a) and its decomposition into sp, ρ_{sp} (b) and d, ρ_d (c) and (d) contributions. All plotted functions are in units of electron/unit cell. Note the change in scale.

Qteish etal. (1995)

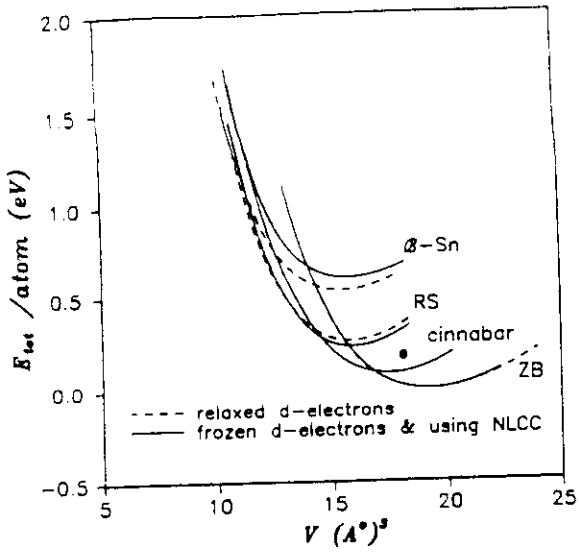

Nazzal ← Qteish

PRB 53, 8262 (1996)

FIG. 1. The calculated EOS's of the ZB, the RS, the β-Sn, and the cinnabar structures of ZnS, using the relaxed d electrons (dashed curves) and the NLCC (solid curves) approaches. The EOS's in the case of the NLCC calculations are rigidly shifted such that the equilibrium total energy, E_{tot}^{eq}, and the equilibrium volume of the ZB structure match the corresponding values of the same structure obtained using the relaxed d electrons approach. Solid circle: E_{tot} of the cinnabar structure calculated using the relaxed d electrons approach at $a=3.8$ Å and its optimal values of c/a, u, and v (which are, in this case, 2.28, 0.46, and 0.49, respectively). The zero energy is taken to be equal to E_{tot}^{eq} of the ZB structure.

TABLE I. Structural parameters of the ZB, the RS, the β-Sn, and the cinnabar structures of ZnS.

Structural parameter	ZB	RS	β-Sn	Cinnabar
a_0 (Å)	5.409,[a] 5.2803,[b] 5.394,[f] 5.413,[c] 4.715,[g] 5.410,[d] 5.186[h] } expt.	5.02,[a] 4.95,[b] 5.06,[c] 5.21,[e] 5.094[f]	4.769,[a] 4.738[b]	3.761[b]
B_0 (GPa)	83.2,[a] 83.3,[b] 75,[c] 76.9,[d] 75.9,[e] 82,[f] 145,[g] 106[h]	104.4,[a] 107.6[b] 103.6,[c] 83.1,[e] 100.1[f]	93.8,[a] 86.7[b]	92[b]
B_0'	4.43,[a] 3.92,[b] 4,[c] 4.9,[d] 4.7,[e] 4.2[f]	4.29,[a] 4.1,[b] 4,[c] 10,[e] 4.05[f]	4.4,[a] 4.96,[b]	3.1[b]
$(c/a)_0$			0.5683,[a] 0.5608[b]	2.3363[b]
u_0				0.455[b]
v_0				0.48[b]

a Relaxed d-electrons

b NLCC ⇒ NR-PP

g Frozen core d-electrons without NLCC.

h as in (b) but with SR-PP